Plant Biotechnology Journal

Plant Biotechnology Journal (2015), pp. 1–12 doi: 10.1111/pbi.12327

Inhibiting plant microRNA activity: molecular *SPONGE*s, target *MIMIC*s and STTMs all display variable efficacies against target microRNAs

Marlene Reichel†, Yanjiao Li†, Junyan Li and Anthony A. Millar*

Plant Science Division, Research School of Biology, Australian National University, Canberra, ACT, Australia

Received 16 September 2014;
revised 9 December 2014;
accepted 10 December 2014.
**Correspondence* (Tel 61 2 612 5870;
fax 61 2 612 5333;
email tony.millar@anu.edu.au)
†joint first authors

Keywords: microRNA, *MIMIC*s, STTMs, molecular *SPONGE*, ΔG free energy.

Summary

Elucidation of microRNA (miRNA) function through a loss-of-function approach has proven difficult due to extensive genetic redundancy among most plant and animal miRNA families. Consequently, miRNA decoy technologies such as target *MIMIC*s (*MIM*s) and short tandem target MIMICs (STTMs) in plants or molecular *SPONGE*s (*SP*s) in animals have been developed to generate loss-of-function phenotypes by perturbing endogenous miRNA activity. To test whether *SP*s can inhibit plant miRNA activity, synthetic *SP* transgenes containing multiple miRNA binding sites targeting different *Arabidopsis* miRNA families were generated. Additionally, their silencing efficacies were compared to the corresponding *MIM* and *STTM* transgenes via scoring the frequency and severity of phenotypic abnormalities elicited by each transgene. While *SP*s with wild-type miRNA binding sites have no apparent impact, *SP*s containing miRNA binding sites with two central mismatches (*cmSP*s) can generate strong loss-of-function phenotypes. However, their efficacy varied dramatically, from inducing strong loss-of-function phenotypes to failing to produce any phenotypic impact. Variability was also observed when *MIM*s and STTMs were compared to *cmSP*s. While *cmSP165/166* and STTM165/166 showed a stronger efficacy than *MIM165/166*, *MIM159* was stronger than *cmSP159* and STTM159. Although increasing the number of miRNA binding sites or strengthening the free energy of the miRNA binding site interaction can improve decoy efficacy, clearly additional unknown overriding factors are at play. In conclusion, we demonstrate that no one approach guarantees the strongest miRNA inhibition, but rather distinct miRNA families respond differently to the various approaches, suggesting that multiple approaches may need to be taken to generate the desired loss-of-function outcome.

Introduction

The discovery of the importance of small noncoding RNAs (sRNAs) in controlling gene expression has led to a paradigm shift in our understanding of the information contained in the genome and how it is regulated. Central to this has been the in-depth elucidation of a class of endogenous 20–24 nucleotides (nt) sRNAs known as microRNAs (miRNAs). They are incorporated into RNA-induced silencing complexes (RISCs), which they guide to complementary mRNAs that are subsequently silenced, mainly through cleavage and translational repression mechanisms (Voinnet, 2009). Cleavage occurs at the phosphodiester bond opposite nt 10 and 11 of the miRNA in the miRNA–mRNA duplex and is catalysed by the RNAse H-like domain of ARGONAUTE (AGO) (Voinnet, 2009). In both plants and animals, miRNAs have been shown to play crucial roles in many different biological processes, including development, disease and environmental responses (Sunkar *et al.*, 2012), making miRNAs strong targets for biotechnology (Zhou and Luo, 2013).

In plants, the biological roles of most miRNAs remain unknown, as accurately defining their function has remained challenging. Much of the functional analysis of miRNAs has been based on gain-of-function approaches that have obvious limitations. Firstly, methodologies using the strong constitutive 35S promoter in activation tagging mutagenesis or miRNA overexpression will generally lead to miRNA expression levels and patterns that are not representative of the *in vivo* condition and therefore may misrepresent the endogenous role of the miRNA (Voinnet, 2009). An alternative approach has been the use of miRNA-resistant target transgenes, but this approach, even when using the target gene promoter, can also potentially misrepresent miRNA function due to transgenic artefacts (Li and Millar, 2013). Therefore, conclusions from these strategies must be drawn with caution and need to be confirmed by miRNA loss-of-function approaches. However, creating loss-of-function *mirna* mutants is problematic as most miRNAs belong to gene families consisting of multiple redundant members, so the generation of combinatorial loss-of-function mutants has only been achieved for miRNA families with few members (Allen *et al.*, 2007; Sieber *et al.*, 2007).

To address this deficiency, a number of transgenic methodologies have been developed that generate loss-of-function outcomes. This has included using artificial miRNAs against endogenous miRNAs, which can target either single or multiple family members (Eamens *et al.*, 2011) or RNAi approaches that target the primary-miRNA transcript and its promoter (Vaistij

Please cite this article as: Reichel, M., Li, Y., Li, J. and Millar, A.A. (2015) Inhibiting plant microRNA activity: molecular *SPONGE*s, target *MIMIC*s and STTMs all display variable efficacies against target microRNAs. *Plant Biotechnol. J.*, doi: 10.1111/pbi.12327

et al., 2010). More widely used has been the transgenic expression of decoy targets, which are RNA molecules with high complementarity to particular miRNA families (Ivashuta *et al.*, 2011; Todesco *et al.*, 2010; Yan *et al.*, 2012). These decoys act by competing for miRNA binding thereby reducing the number of miRNAs available for the repression of primary targets, which results in their deregulation. In plants, transcripts that contain a single noncleavable miRNA binding site called target *MIMIC*s (*MIM*s) can act as such decoys. *MIM*s are based on the nonprotein coding gene *INDUCED BY PHOSPHATE STARVATION 1* (*IPS1*) that inhibits miR399 (Franco-Zorrilla *et al.*, 2007). *IPS1* contains a highly complementary binding site for miR399 but has a 3 nt mismatch loop at the miRNA cleavage site. Due to this loop, it is thought that *IPS1* cannot be cleaved but instead sequesters the miR399-loaded RISC leading to the de-repression of the primary-miRNA target gene (Franco-Zorrilla *et al.*, 2007). The *IPS1* gene was modified to generate 73 artificial *MIM*s to individually inhibit the majority of known miRNA families in *Arabidopsis*. From this experiment, the expression of 15 *MIM*s resulted in obvious morphological phenotypes, some of which were similar to phenotypes caused by expressing the corresponding miRNA-resistant target gene or the corresponding miRNA loss-of-function mutant (Todesco *et al.*, 2010).

As some *MIM*s did not generate strong loss-of-function phenotypes, short tandem target mimics (STTMs), composed of two *MIM* binding sites separated by a 48 nt spacer, were generated as a subsequent modification of the *MIM* approach (Yan *et al.*, 2012). STTMs were optimized against the miRNA family miR165/166, and it was empirically determined that a spacer of 48 nt and the two binding sites are both required for strong miR165/166 inhibition, generating a stronger phenotype than a *MIM165/166* decoy. This STTM design was then applied to two other miRNA families, miR156/157 and miR160, and two transacting small interfering RNAs and in each case produced strong loss-of-function phenotypes, indicating the robustness of the approach. However, although the STTM165/166 resulted in complete destruction of miR165/166 (Yan *et al.*, 2012), Arabidopsis plants expressing a STTM396 only had moderately decreased miR396 levels (Liang *et al.*, 2014) suggesting that the efficacy of the approach may vary depending on the miRNA targeted.

In animal systems, the use of 'miRNA sponges' has proven very effective at inhibiting miRNA action (Ebert *et al.*, 2007). Sponges (*SP*s) are synthetic transcripts that contain multiple binding sites to a miRNA of interest, either in a nonprotein coding RNA or in the 3' UTR of a reporter gene. They compete for miRNA binding, which results in the perturbation of the endogenous miRNA–target mRNA interaction. As their specificity is mainly determined by the degree of complementarity to the miRNA, they are able to target entire miRNA families and thus, like plant *MIM*s or STTMs, can overcome problems of functional redundancy due to multiple miRNA family members. Although *SP*s with perfect complementarity to a miRNA were shown to inhibit miRNA activity to some extent, *SP*s with bulges to positions 9–12 of the target miRNA had a greater efficacy (Ebert *et al.*, 2007).

Here, we have investigated the use of miRNA *SP*s, synthetic transcripts with multiple miRNA binding sites as a methodology for inhibiting miRNA action in plants. We found that *SP*s containing 15 miRNA binding sites with mismatches at the cleavage site (*cmSP*s) could strongly perturb miRNA activity; however, their efficacies varied dramatically depending on the miRNA family targeted. Likewise, from direct comparisons of *cmSP*s to *MIM*s and STTMs, we found that the silencing efficacy of *MIM*s and STTMs also varies, demonstrating that different miRNA families respond differently to the three approaches and that no one approach works equally well for the miRNAs tested.

Results

Design of miRNA *SPONGES* to target the miR159 and miR165/166 families

Firstly, we generated *SP*s that aimed to specifically perturb miR159 and miR165/166. *SP*s were designed largely according to Ebert *et al.* (2007), where they have multiple miRNA binding sites separated by 4 nt spacers. Furthermore, they contained unique primer binding sites which were used for measuring *SP* transcript levels by qRT-PCR (Figure 1a). All *SP* constructs were under the transcriptional control of a dual 35S CaMV promoter in the binary vector pMDC32 (Curtis and Grossniklaus, 2003), to enable strong constitutive expression. *SP*s with two types of miRNA binding sites were created for both miR159 and miR165/166. Firstly, to investigate the impact of endogenous target site abundance on miRNA regulation, *SP*s containing binding sites identical to the endogenous miRNA binding sites of the targets of miR159 (*MYB33/65*) or miR165/166 (*PHB/PHV*) were made [termed wild type (*wt*) *SP159* and *wtSP165/166*]. Secondly, to examine the role of cleavage, *SP*s containing binding sites with mismatches at the cleavage site, which is opposite nts 10–11 of the respective miRNA, were generated [termed central mismatch (*cm*) *SP159* and *cmSP165/166*] (Figure 1b,c). *CmSP*s are different from the original *SP*s by Ebert *et al.* (2007), which contained a bulge at the cleavage site as opposed to two central mismatches. *WtSP*s contained fifteen miRNA binding sites, whereas *cmSP*s contained three (3×), seven (7×) or fifteen (15×) miRNA binding sites, respectively. In contrast to *MIM*s and STTMs, *SP*s contain no additional nts between position 10 and 11, hence no asymmetric mismatch loop forms at the cleavage site when bound with respective miRNAs.

WtSP165/166 and *cmSP165/166* were transformed into wild-type (Col-0) *Arabidopsis* plants, while *wtSP159* and *cmSP159* were transformed into wild-type and *mir159a* mutant plants. The *mir159a* allele is a strong loss-of-function mutant, where total miR159 levels are reduced to approximately 10% of wild type (Allen *et al.*, 2010). Hence, the use of wild-type and *mir159a* plants enables the impact of miRNA abundance on the efficacy of the *SP*s to be ascertained. The *GUS* reporter gene, cloned into the same vector as the *SP*s, was used as a transgenic control.

A *cmSP159* transgene can strongly inhibit miR159 activity

To evaluate the efficacy of miRNA inhibition by the transgene, the frequency and severity of morphological defects were scored for multiple independent primary transformants of the same construct. For *SP159* analysis, primary transformants were grown side-by-side and classified as having weak (leaf curling with little or no growth reduction), moderate (leaf curling with growth reduction) or severe (leaf curling with strong reduction in size similar to a strong loss-of-function *mir159ab* double mutant; Figure 2a) phenotypes.

All *wtSP159* (Col-0), *wtSP159* (*mir159a*) and *cmSP159* (3×) primary transformants were indistinguishable from wild type. In contrast, 64% (74 of 116) of *cmSP159* (7×) and 79% (84 of 106) of *cmSP159* (15×) primary transformants displayed moderate and

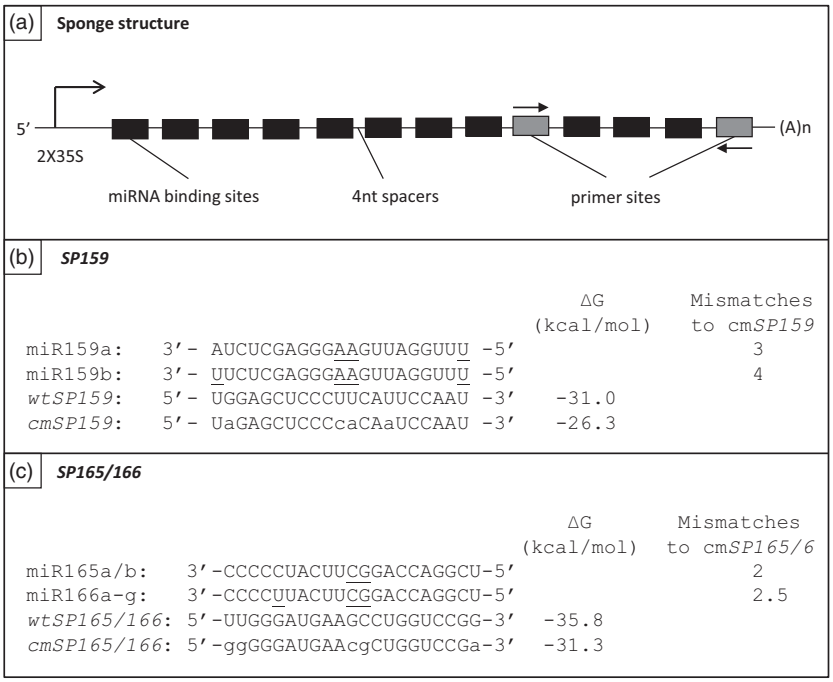

Figure 1 Structure and sequences of *SP159*, *SP165/66* and their corresponding targeted miRNAs. (a) *SP*s are composed of multiple miRNA binding sites separated by 4 nt spacers and two unique sequences that serve as priming sites for qRT-PCR. They are driven by a dual 35S promoter and harbour a poly(A) tail. (b) *wtSP159* contains binding sites that are identical to the endogenous miR159 binding site in *MYB33/65*, while *cmSP159* contains binding site with mismatches at the cleavage site (lower case). The endogenous mismatches have been corrected to maintain a similar free energy (ΔG). *SP159* can target both miR159a and miR159b. (c) *wtSP165/166* contains binding sites that are identical to the endogenous miR165/166 binding site in *PHB/PHV*, while *cmSP165/166* contains mismatches at the cleavage site. Original mismatches have been corrected to minimize changes in free energy (ΔG). Tables indicate ΔG values and the number of mismatches to the corresponding *cmSP* (mismatched nucleotides are underlined). ΔG values were calculated using the DINAmelt Web Server (http://mfold.rna.albany.edu/?q=DINAMelt/Two-state-melting).

weak phenotypes (Figure 2b). *CmSP159* (15×) caused stronger effects than *cmSP159* (7×), as a higher percentage of plants showed a moderate phenotype; however, neither construct could induce severe phenotypes as observed in *mir159ab*. *CmSP159* (15×) showed a better efficacy in *mir159a* where 76% (65 of 86) of plants displayed moderate phenotypes, compared to Col-0 plants with only 25% (27 of 106) of plants showing moderate symptoms (Figure 2c). Thus, the efficacy of *cmSP159* appears to be influenced by both the abundance of miR159 and the number of miRNA binding sites. All GUS transformants had a wild-type phenotype (Figure 2a).

As *cmSP159* (15×) had the strongest efficacy, we decided to further test its impact and that of *wtSP159* on miR159 regulation by measuring transcript levels of its target genes, *MYB33* and *MYB65*, and the downstream gene *CP1,* which acts as a marker for MYB33/65 protein activity (Alonso-Peral *et al.*, 2010). For *MYB33/MYB65*, gene-specific primers spanning the miRNA binding site were used to quantify intact (unsliced) target mRNA. Consistent with previous studies (Allen *et al.*, 2007), the mRNA levels of *MYB33* and *MYB65* were ~fivefold and ~sevenfold higher, respectively, in *mir159ab* than in wild-type plants (Figure 2d). In *wtSP159* (Col-0) plants, *MYB33* and *MYB65* transcript levels remained unchanged compared to the controls, which was also reflected in the unaltered *CP1* levels. For *wtSP159* (*mir159a*) plants, *MYB33*, *MYB65* and *CP1* transcript levels were ~1.5- to 2-fold higher compared to the controls (Figure 2d). Thus, *wtSP159* may be having an effect on miR159 silencing in *mir159a* plants; however, any perturbation of miR159 activity is not strong enough to enable deregulation of MYB33 or MYB65 expression to levels resulting in a phenotypic impact. By contrast, *cmSP159* (15×) plants had strong increases in *MYB33* and *MYB65* transcript abundance. Similarly, *CP1* transcript levels were higher compared to the wild-type and *GUS* controls (Figure 2d). A clear positive correlation was observed between the target transcript levels and the corresponding phenotypes, where plants exhibiting moderate (M) developmental defects had higher transcript levels than plants with weak (W) phenotypes.

Next, qRT-PCR was used to examine the *SP* transcript levels. The level of *cmSP159* (15×) was considerably higher than that of *wtSP159* (Figure 2d), presumably because slicing of *cmSP159* transcripts is attenuated, enabling a higher level of *SP* accumulation. The abundance of *cmSP159* (15×) transcripts was positively correlated with phenotypic severity, as *cmSP159* (15×) plants with moderate phenotypes showed higher *cmSP159* RNA levels compared to the corresponding plants with weak phenotypes (Figure 2d). The abundance of *cmSP159* (15×) was lower in *mir159a* compared to Col-0, although the phenotypes were more severe in the former. This is likely due to the fact that *mir159a* plants have greatly reduced miR159 levels and thus require less *SP* RNA to achieve strong perturbation of miR159 activity.

To investigate whether miRNA abundances are affected by *SP* expression, TaqMan miRNA assays were performed to estimate mature miR159 levels. A negative correlation between *SP159* levels and miR159 abundance was observed. In *wtSP159* (Col-0) plants, miR159 levels were similar to wild-type levels, whereas *cmSP159* (15×) (Col-0) plants showed significantly decreased miR159 levels (Figure 2d).

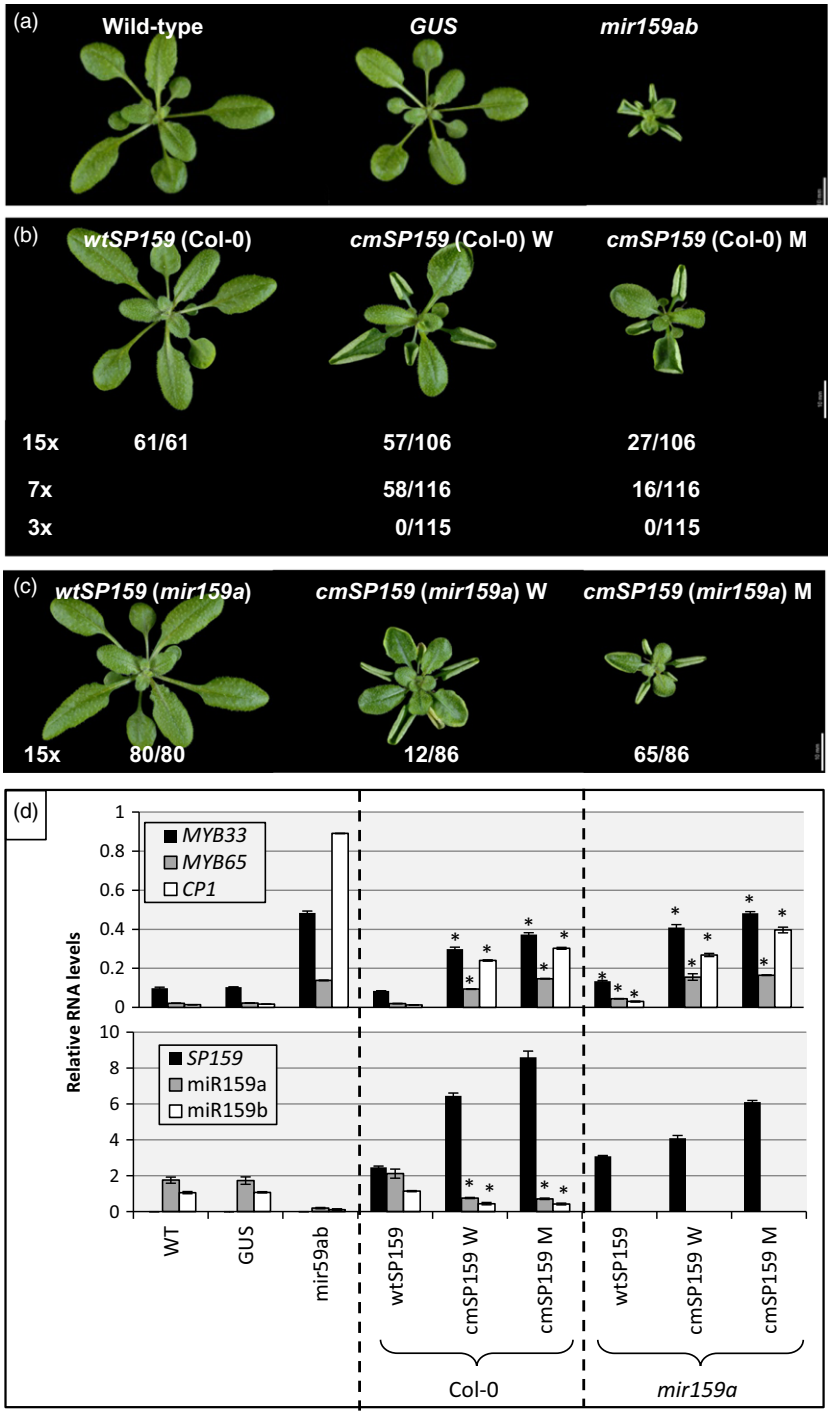

Figure 2 Phenotypic and molecular analysis of 4-week-old *Arabidopsis* plants expressing *wtSP159* and *cmSP159*. (a) Wild-type (Col-0) plants and plants expressing the *GUS* gene were used as negative controls, while *mir159ab* was used as a positive control**.** Col-0 (b) and *mir159a* plants (c) expressing *wtSP159* and *cmSP159*. M: moderate, W: weak phenotype. 3×, 7×, 15×: three, seven, fifteen miRNA binding sites, respectively. Numbers indicate the portion of primary transgenic lines falling into the phenotypic class shown. Scale bar = 10 mm. (d) qRT-PCR analysis of target transcript, miRNA and *SP* levels in *wtSP159* and *cmSP159* (15×) plants. *MYB33, MYB65*, *CP1* and *SP*159 levels were measured relative to *CYCLOPHILIN*, and TaqMan assays of mature miR159a and miR159b levels were normalized to *snoR101*. RNA was extracted from 4-week-old primary transformants using tissue from whole plants. Measurements are the average of three technical replicates with error bars representing the SEM. Asterisks mark statistically significant changes compared to the negative controls as determined by Student's *t*-test analysis.

A *cmSP165/166* transgene strongly perturbs miR165/166 activity

Similar to *wtSP159*, expression of *wtSP165/166* did not result in any phenotypic abnormalities. However, 103 of 105 *cmSP165/166* (15×) and 75 of 92 *cmSP165/166* (7×) primary transformants displayed phenotypic abnormalities of adaxialized leaves (Figure 3a), the expected phenotype of a miR165/166 loss-of-function mutant (Xu *et al.*, 2007). Plants were classified as having weak (weakly adaxialized organs), moderate (strongly adaxialized organs) or severe (trumpet- and cup-shaped leaves with fasciated stems and flowers) phenotypes. Moderate and severe lines were sterile, and the latter did not produce extended internodes in the inflorescence resulting in floral clumps (Figure S1a). *CmSP165/166* (15×) clearly showed the strongest efficacy with 75 of 105 plants showing severe abnormalities, whereas of 92 *cmSP165/166* (7×) transformants, two showed severe, 17 showed moderate and 56 showed weak symptoms. *CmSP165/166* (3×) did not appear to be able to strongly perturb miRNA activity, as only 3 of 121 transformants showed weak defects, while all other transformants had no phenotypic abnormalities.

Next, transcript levels of the miR165/166 target genes *PHB, PHV* and *ATHB-15* (Emery *et al.*, 2003; McConnell *et al.*, 2001)

were measured in *wtSP165/166* and *cmSP165/166* (15×) plants using qRT-PCR. Consistently, the transcript levels of these genes were slightly elevated in *wtSP165/166* plants, but were strongly up-regulated in *cmSP165/166* (15×) plants (Figure 3b), strongly correlating with the morphological defects. Additionally, transcript levels of *cmSP165/166* (15×) were higher than that of *wtSP165/166* and positively correlated with phenotypic severity (Figure 3b). Together, these data demonstrate that *cmSP*s with 15 miRNA binding sites are most effective in inhibiting miRNA activity.

Utilization of *cmSP165/166* to inhibit miR165/166 function in a tissue-specific manner

As many plant miRNAs are known to be expressed in a spatiotemporal manner, it is often of interest to analyse miRNA function in a specific tissue. Thus, we aimed to test whether *cmSP*s can be used for tissue-specific inhibition of miRNA activity. To do this, *cmSP165/166* (15×) was cloned downstream of the pOp6 promoter (pOp6-*cmSP165/166*) to utilize the pOp6/LhG4 transactivation system (Figure 4a) (Craft *et al.*, 2005). The pOp6-*cmSP165/166* construct as well as a pOp6-GUS control were then transformed into the LhG4 enhancer trap line HET:59a (Rutherford *et al.*, 2005). As shown by GUS staining (Figure 4b), transgene expression in the HET:59a line occurs predominantly in the shoot apical region (SAR) and young petioles. Expression of *cmSP165/166* in these tissues induced strong developmental defects in leaves and floral tissues. Primary pOp6-*cmSP165/166* transformants showed ectopic growth of fasciated flowers resembling the floral phenotype induced by *cmSP165/166* under the 35S promoter (Figure 4f). Furthermore, an outgrowth of adaxial-like tissue with trichomes was apparent on the abaxial side of the leaf, which was not observed in plants constitutively expressing *cmSP165/166* (Figure 4d,e). These phenotypes indicate that using the pOp6/LhG4 system, we have successfully expressed *cmSP165/166* in a spatial manner generating a tissue-specific miR165/166 loss-of-function phenotype.

Application of *cmSP*s targeting different miRNAs reveals varying efficacy

To further test the applicability of *cmSP*s as miRNA inhibitors, additional *35S-cmSP* (15×) transgenes were generated aiming at specifically inhibiting individual miRNA families.

Firstly, of 42 primary transformants generated with a *cmSP164* transgene, four plants showed moderate defects characterized by serrated rosette leaves (Figure 5a), which is similar to the phenotype reported for a *mir164abc* triple mutants (Sieber *et al.*, 2007). However, the disruption of phyllotaxis and floral organ development as seen in *mir164abc* was not evident in *cmSP164* transformants indicating that miR164 activity might not be completely inhibited.

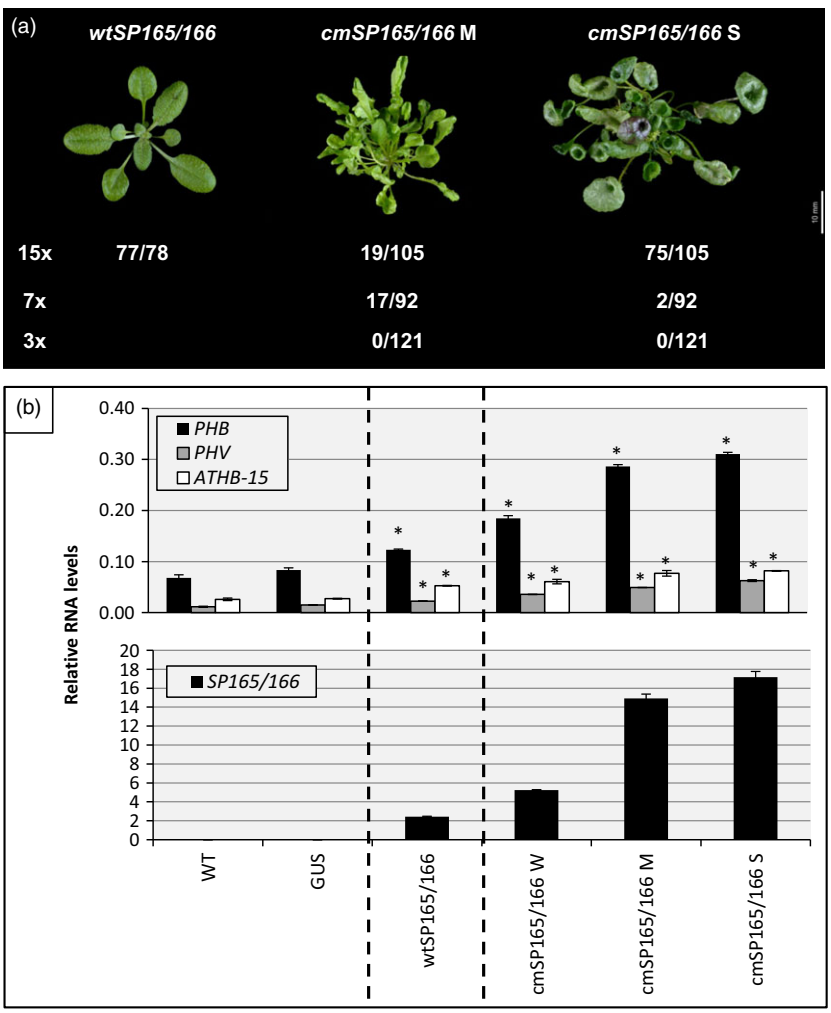

Figure 3 Phenotypic and molecular analysis of 4-week-old *Arabidopsis* plants expressing *wtSP165/166* and *cmSP165/166*. (a) Col-0 plants expressing *wtSP165/166* and *cmSP165/166.* M: moderate, S: severe phenotype. 3×, 7×, 15×: three, seven, fifteen miRNA binding sites, respectively. Numbers indicate the portion of primary transgenic lines falling into the phenotypic class shown. Scale bar = 10 mm. (b) qRT-PCR analysis of target transcript and *SP* levels in *wtSP165/166* and *cmSP165/166* (15×) plants. *PHB, PHV, ATHB-15* and *SP*165/166 levels were measured relative to *CYCLOPHILIN*. RNA was extracted from 4-week-old primary transformants using tissue from whole plants. Measurements are the average of three technical replicates with error bars representing the SEM. Asterisks mark statistically significant changes compared to the controls. W: weak, M: moderate, S: severe phenotype.

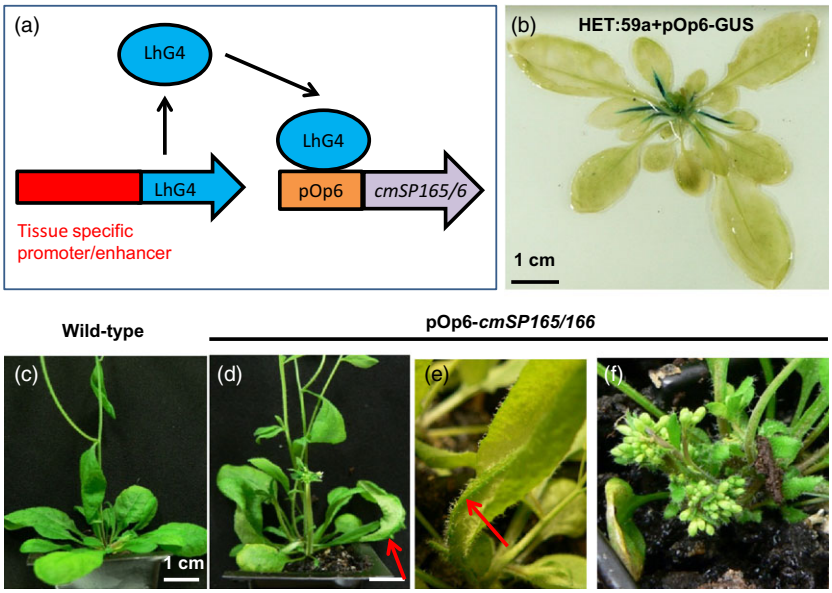

Figure 4 Generation and phenotypic analysis of pOP6-*cmSP165/166* (HET:59a) transgenic plants. (a) Cartoon depicting the transactivation of pOP6-*cmSP165/166* by LhG4. (b) Histochemical GUS staining in 40-day-old rosettes of pOP6-GUS (HET:59a) control plants. (c and d) Phenotypic comparison of 5-week-old wild-type (pOP6-GUS (HET:59a)) plants and pOP6-*cmSP165/166* (HET:59a) plants. (e and f) Close-up of defects in leaves and floral organs typical of 5-week-old pOP6-*cmSP165/166* (HET:59a) transformants. Red arrows indicate adaxial tissue growing on the abaxial side of leaves in pOP6-*cmSP165/166* (HET:59a) transformants.

Next, of 50 primary transformants expressing a *cmSP390* transgene, 29 showed developmental defects characterized by narrow leaves and downwardly curled leaf margins. Two plants also appeared smaller in rosette size and were thus classified as severe (S), while the other 27 plants showing leaf defects were classified as moderate (M) (Figure 5b). These morphological phenotypes resemble that of the *ago7* mutant. AGO7 specifically loads miR390 and triggers the production of transacting siRNAs (tasiRNAs), which regulate *AUXIN RESPONSE FACTOR* (*ARF*) genes controlling leaf development (Adenot *et al.*, 2006; Garcia *et al.*, 2006; Hunter *et al.*, 2006). Consistently, transcript levels of *ARF3* and *ARF4* were significantly increased in *cmSP390* S plants compared to Col-0, while no changes were observed in *cmSP390* plants that did not display a mutant phenotype (NP). Thus, both the molecular and morphological phenotypes indicate that *cmSP390* could inhibit miR390 activity.

However, other *cmSP* (15×) transgenes which would be predicted to result in strong developmental defects failed to generate any transgenic plants displaying the predicted phenotype. For instance, *cmSP156* (15×) and *cmSP172* (15×) transgenes failed to result in any phenotype (>30 primary transformants; data not shown), despite other approaches successfully generating strong loss-of-function phenotypes when targeting these miRNAs (Todesco *et al.*, 2010; Yan *et al.*, 2012). Therefore, the *SP* approach appears highly variable in its ability to inhibit miRNA-mediated activities, where strong (*cmSP166*, *cmSP159*), weak (*cmSP164*, *cmSP390*) and no (*cmSP156*, *cmSP172*) inhibition occurred for different target miRNAs.

CmSP165/166 and *STTM165/166* have a stronger efficacy than *MIM165/166*

To appraise the efficacy of *cmSPs* (15×), they were compared to other decoy technologies such as *MIMs* and STTMs (Todesco *et al.*, 2010; Yan *et al.*, 2012). All decoys were subcloned into pMDC32 that contains the dual 35S promoter, the same binary vector backbone as the *cmSPs*, enabling direct efficacy comparisons through analysis of multiple independent primary transformants for each construct.

Firstly, we compared the efficacies of *cmSP165/166*, *MIM165/166* and STTM165/166 by scoring the severity and frequency of developmental abnormalities (leaf adaxialization; Figure 6a) in multiple independent primary transformants for each construct. For *cmSP165/166,* the majority (64%) of primary transformants displayed a severe phenotype (Figure 6b). By contrast, none of the *MIM165/166* plants displayed such a phenotype, but mainly displayed moderate and weak phenotypes based on the classification (Figure 6b). Consistent with this, the miR165/166 target transcripts *PHB, PHV* and *REV* were much higher in *cmSP165/166* than in *MIM165/166* plants (Figure S2). The previously reported STTM165/166-48 (a *MIM165* and *MIM166* binding site in tandem separated by a 48 nt spacer) conferred a strong efficacy with 24% of 82 primary transformants showing a severe phenotype (Figure 6b), an efficacy similar to what was previously reported, where 30% of primary transformants resulted in strongly adaxialized leaves (Yan *et al.*, 2012).

The number of miRNA binding sites and the strength of ΔG interaction influence decoy efficacy

To test whether the higher efficacy of *cmSP165/166* and STTM165/166-48 compared to *MIM165/166* is due to the increased number of miR165/166 binding sites or the sequence of the binding sites, we generated a *SP* construct with 15 *MIM165/166* binding sites [*SP165/166* (15× MIM)]. Furthermore, the miRNA binding site of *MIM165/166* has an additional mismatch to miR165/166 when compared to the binding sites of STTM165/166-48 (Figure S3) resulting in a weaker ΔG interaction (Table S1). Hence, another *SP* construct containing 15 *MIM165/166* sites with this mismatch corrected (MIM-MC) was also generated [named *SP165/166* (15× MIM-MC)] to test whether strengthening the ΔG interaction can increase efficacy.

For *SP165/166* (15× MIM), approximately 9% of 90 primary transformants displayed a severe phenotype implying it has a stronger efficacy than *MIM165/166* (Figure 6b). This indicates that increasing the number of miRNA binding sites can increase efficacy. Additionally, for *SP165/166* (15× MIM-MC), approximately 14% of 99 primary transformants displayed a severe phenotype (Figure 6b), suggesting it has a stronger efficacy than *SP165/166* (15× MIM) and that the increase of the ΔG interaction increases decoy efficacy.

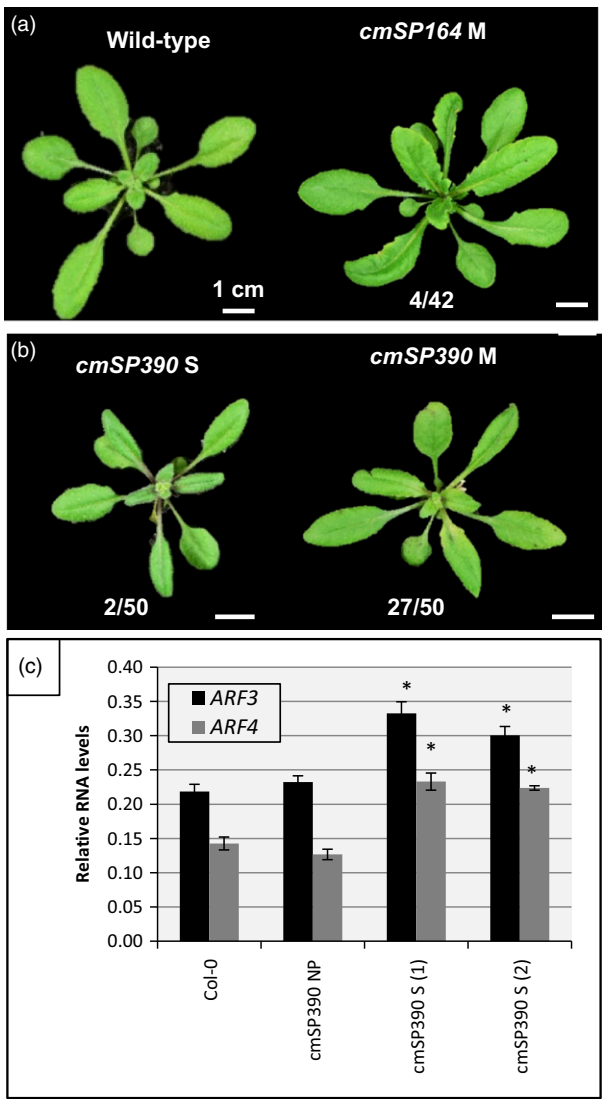

Figure 5 Analysis of 4-week-old *Arabidopsis* plants expressing *cmSP164* and *cmSP390*. Aerial view of wild-type (Col-0) plants (a), *cmSP164* plants (b) and *cmSP390* plants (c). S: severe, M: moderate phenotype. Numbers indicate the portion of primary transgenic lines showing developmental defects. Scale bar = 10 mm. (d) qRT-PCR analysis of *ARF3* and *ARF4* transcript levels in the rosettes of the progeny of the primary transformants (T2). RNA was extracted from rosettes of 5-week-old plants classified according to their phenotype. mRNA levels were normalized to *CYCLOPHILIN*. Measurements equal the average of three technical replicates with error bars representing the SEM. Asterisks mark statistically significant changes compared to the controls. S: severe, NP: no phenotype.

However, the efficacy of *SP165/166* (15× MIM-MC) is still considerably weaker than the efficacy of STTM165/166-48, which only has two miRNA binding sites, and that of *cmSP165/166* (15×), which contains a binding site with two central mismatches rather than a 3 nt loop (Figure S3). Therefore, although increasing the number of miRNA binding sites or strengthening the ΔG interaction may improve decoy efficacy, clearly other factors are having a major impact.

To test the effect of the different decoys on miRNA levels, we measured miR166a levels in primary transformants classified according to their phenotype. Consistent with previous measurements, a tight negative correlation between phenotypic severity and miRNA levels can be observed for all decoy constructs. While miR166a levels in decoy plants showing no and mild phenotypes are similar to wild type, they are strongly reduced in plants with moderate and severe phenotypes (Figures 6c, S2).

MIM159 has an efficacy stronger than *cmSP159* and STTM159

To appraise the efficacy of *cmSP159* (15×), it was compared to *MIM159* (Todesco *et al.*, 2010) and STTM159, which contained two *MIM159* binding sites separated by a 48 nt spacer (based on the design from Yan *et al.*, 2012). All constructs were cloned into pMDC32 and transformed into Col-0; *MIM159* was also transformed into *mir159a*.

Primary transformants were grown side-by-side and classified as having weak, moderate or severe phenotypes (Figure 7a), using the criteria described before. In accordance with previous results, none of the *cmSP159* (15×) transformants displayed severe defects. In contrast, approximately 50% *MIM159* (Col-0) and *MIM159* (*mir159a*) transformants showed severe abnormalities, with strong leaf curl and stunted growth (Figure 7b), implying that *MIM159* has a stronger efficacy than *cmSP159* (15×). However, STTM159 was also unable to induce severe phenotypes, where its efficacy also appeared weaker than that of *cmSP159* (15×), as only approximately 1% (one of 82) of STTM159 primary transformants displayed moderate phenotypes. This shows that *MIM159* is considerably more potent in inhibiting miR159 than both STTM159 and *cmSP159* (15×), again demonstrating that the number of miRNA binding sites does not necessarily determine the efficacy of miRNA inhibition. Finally, measurement of miR159a levels demonstrates the negative correlation between miRNA levels and phenotypic severity, where the stronger the phenotype, the stronger the reduction in miR159 levels (Figure 7c).

Discussion

Here, we have demonstrated that molecular *SP*s with multiple miRNA binding sites can be effective inhibitors of miRNA activity and thus represent a strategy in plants for generating strong loss-of-function miRNA phenotypes. Moreover, we have evaluated the efficacies of different technologies used for inhibiting miRNA activity, *cmSP*s, *MIM*s and *STTM*s, and have found that no one approach guarantees the strongest inhibition, but rather their efficacies can vary dramatically depending on the miRNA family targeted. As the reasons for this variation are unclear, we suggest that multiple approaches should be used when attempting to inhibit a plant miRNA family, thus increasing the likelihood of a strong loss-of-function outcome.

*CmSP*s can strongly perturb miRNA action

By generating multiple transformants for any given construct and then measuring the severity and frequency by which they induced a miRNA loss-of-function phenotype, we quantitatively measured the efficacy of each decoy construct. As all constructs were in the same vector backbone (pMDC32) and driven by the same promoter (2 × 35S promoter) (Curtis and Grossniklaus, 2003), differences observed should be independent of transcription.

It was found that *cmSP*s (15×) were able to generate loss-of-function phenotypes, albeit with varying efficacies. Additionally, these *cmSP*s (15×) appeared to work better than existing

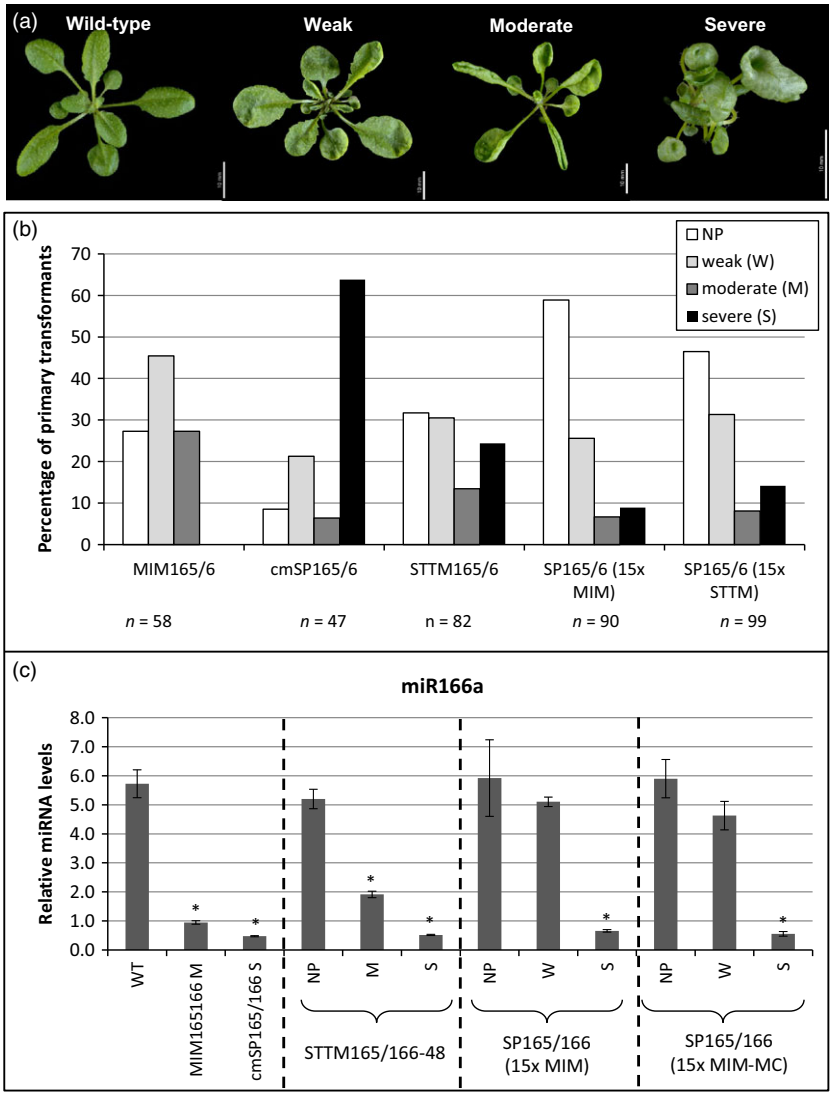

Figure 6 Phenotypic analysis of different decoy constructs targeting miR165/166. (a) Rosette tissue of 4-week-old wild-type (Col-0) plants and representative examples of 4-week-old primary transformants having a weak, moderate or severe phenotype. Scale bar = 10 mm (b) Percentage of primary transformants of different decoys falling into the respective phenotypic categories. All plants were grown side-by-side under the same conditions. *n* = number of primary transformants analysed. (c) qRT-PCR analysis of miR166a levels, normalized to *snoR101,* in different decoys. RNA was extracted from 4-week-old rosette tissue.. Measurements are the average of three technical replicates with error bars representing the SEM. Asterisks mark statistically significant changes compared to wild type. NP: No phenotype, W: weak, M: moderate, S: severe phenotype; MIM-MC: MIM mismatch corrected.

approaches for some miRNA families. For instance, the *cmSP165/166* could strongly inhibit miRNA activity at a frequency greater than *MIM165/166* or STTM165/166-48, and a *cmSP390* (15×) could induce loss-of-function phenotypes, whereas no phenotype was reported for a *MIM390* construct (Todesco *et al.*, 2010). This latter finding demonstrates that *cmSP*s can inhibit miRNAs that are incorporated into AGOs other than AGO1.

By contrast, expression of *wtSP*s at levels many fold higher than endogenous miRNA target transcripts does not appear to impact miRNA action. This implies that efficiently cleaved endogenous plant miRNA targets are unlikely to act as competitive inhibitors against one another. Supporting this is our recent report showing that the stoichiometric ratio of a miRNA:target interaction only becomes important when cleavage has been attenuated (Li *et al.*, 2014). Therefore, it is clear that targets in which miRISC recycling is attenuated have the highest chance of perturbing miRNA activity (Franco-Zorrilla *et al.*, 2007; Poliseno *et al.*, 2010).

*CmSP*s, *MIM*s and *STTM*s all display varying efficacies

By directly comparing the silencing efficacy of *MIM*s, *STTM*s and *cmSP*s, we clearly show that all three approaches are variable in their effectiveness in the inhibition of miRNA-mediated activity. For instance, although *cmSP165/166* (15×) and STTM165/166 were more effective at inhibiting miR165/166 than *MIM165/166*, *MIM159* was more effective at inhibiting miR159 than both *cmSP159* and STTM159 (Figure 7). Additionally, it has been reported that *MIM156* is highly efficient at inhibiting miR156 (Wu *et al.*, 2009), and a STTM156 transgene can also induce strong phenotypes (Yan *et al.*, 2012), whereas a *cmSP156* construct failed to induce any phenotypic defects. Therefore, from this study of the efficacy of multiple approaches targeting multiple miRNA families, it is clear that no one approach guarantees the strongest outcome. Most unexpected was the weak efficacy of the STTM159; the general rules for STTM design were followed [two MIM159 binding sites linked by the empirically determined 48 nt spacer of identical sequence to Yan *et al.* (2012)]; however, the STTM159 had a much weaker efficacy than both *MIM159* and *cmSP159*. This weaker efficacy also strongly contrasts to the robust silencing outcomes of other STTMs, which has been reported (Yan *et al.*, 2012). Similarly, *MIM165/166* appears weak by comparison to many other *MIM*s targeting different miRNA families (Todesco *et al.*, 2010), which again suggests strong variation in any one given method. Therefore, this raises the question of why these approaches vary so dramatically against

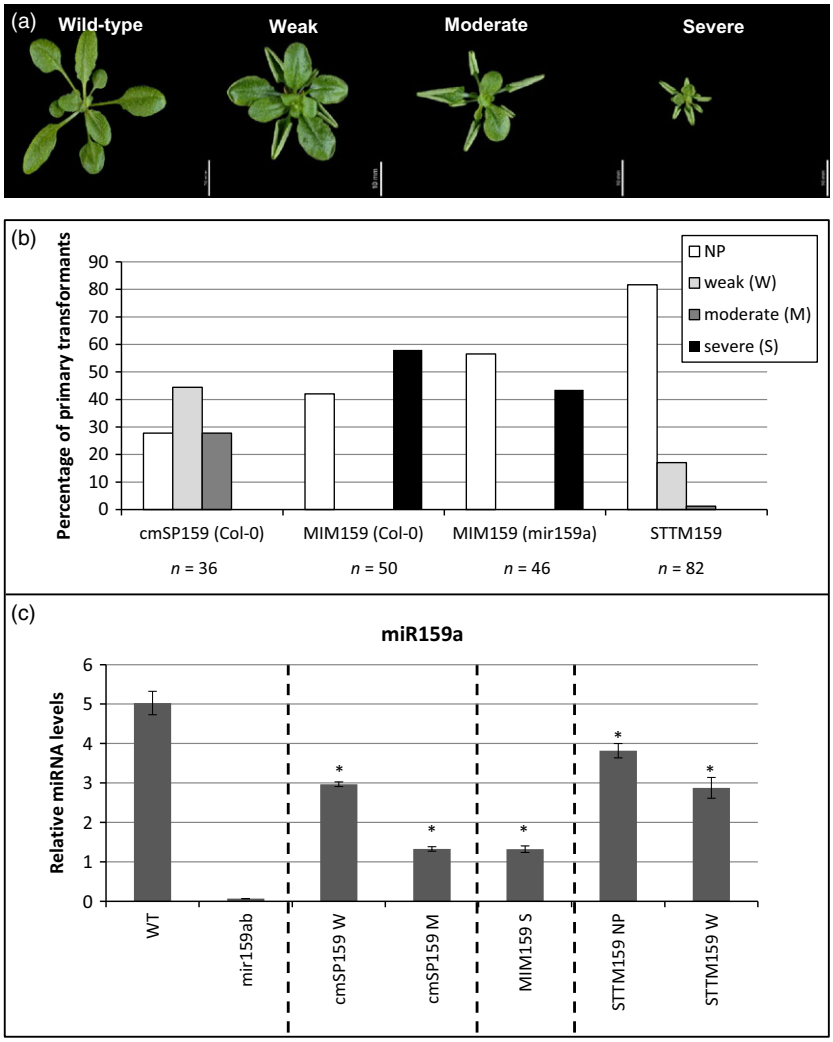

Figure 7 Phenotypic analysis of different decoy constructs targeting miR159. (a) Rosette tissue of 4-week-old wild type (Col-0) and representative examples of 4-week-old primary transformants having a weak, moderate or severe phenotype. Scale bar = 10 mm. (b) Percentage of primary transformants of different decoys falling into the respective phenotypic categories. All plants were grown side-by-side under the same conditions. *n* = number of primary transformants analysed. (c) qRT-PCR analysis of miR159a levels, normalized to *snoR101,* in different decoys. RNA was extracted from 4-week-old rosette tissue. Measurements are the average of three technical replicates with error bars representing the SEM. Asterisks mark statistically significant changes compared to wild type. NP: No phenotype, W: weak, M: moderate, S: severe phenotype.

different miRNA families and what the factors controlling these variable efficacies are.

Factors influencing decoy efficacy

Firstly, a strong ΔG interaction between the miRNA and its target has been shown to be an important determining factor in miRNA target recognition in plants, where a strong ΔG value is a strong determinant of specificity (Schwab *et al.*, 2005). On the one hand, a strong ΔG interaction would facilitate target recognition that would be considered beneficial, but on the other hand, it may encourage cleavage even with two central mismatches as would be the case for *SP*s, preventing miRISC sequestration. In this regard, a target site with a 3 nt loop, opposite nt 10 and 11, as incorporated into *MIM*s and STTMs, would be clearly beneficial, leading to a combination of a noncleavable binding site with a strong ΔG interaction and this is what appears to occur naturally in plants (Franco-Zorrilla *et al.*, 2007; Wu *et al.*, 2013).

Interestingly, the ΔG interaction between the miR165/166 and the different approaches somewhat correlates with their efficacy; the *MIM165/166* has the poorest ΔG (−26.9 kcal/mol), while both *cmSP165/166* and STTM165/166-48 have stronger ΔG values (−31.3 kcal/mol and −35.5 kcal/mol, respectively). The fact that the *MIM165/166* contains a T:C mismatch at nt position 11 of the miRNA that was changed to a G:C pair in STTM165/166-48 (Figure S3) underlies the difference in ΔG values and possibly contributes to the poor efficacy of *MIM165/166*. This is supported by the observation that repairing this mismatch resulted in a slightly stronger efficacy in *SP165/166* (15× STTM) compared to *SP165/166* (15× MIM) (Figure 6). Continuing this trend, *MIM159* (−28.8 kcal/mol) has a stronger ΔG to miR159 than the *cmSP159* (−26.3 kcal/mol). Such data argue that ΔG values are a factor worth taking into account when designing such constructs.

However, it is clear that the ΔG value is not an absolute indicator of efficacy as highlighted by the *MIM159* having a much greater efficacy than STTM159 despite both having identical miR159 binding sites. Additionally, in rice, a *MIM* that had two mismatches against an artificial miRNA (amiRNA) conferred a stronger efficacy than a *MIM* with no mismatches (Chen *et al.*, 2013). Therefore, factors beyond complementarity must be contributing to decoy efficacy. One obvious factor could be the stability of the decoy transcript; for instance, many natural *SP* transcripts in animals are circular, which may increase their resistance to degradation (Hansen *et al.*, 2013). Although all decoys analysed in this study were in the same vector backbone, meaning that the transcription rate should not be a differential factor, it is possible that the different decoy transcripts have different RNA stabilities.

Another likely factor is RNA secondary structure. In the development of the STTM technology, Yan *et al.* (2012) have

shown that the length of the DNA spacer between the two *MIM* sites is predicted to influence secondary RNA structure, which was hypothesized as a contributing factor to the strong efficacy of STTM165/166. For instance, increasing the spacer length of the STTM165/166 from 48 nt to 88–96 nt increases the frequency of transgenic plants with a severe phenotype from approximately 30% to over 60% (Yan *et al.*, 2012). However, even if the spacer sequence is identical between different STTMs targeting different miRNAs, the sequence of the miRNA binding sites will vary, likely resulting in altered RNA secondary structures as based on *in silico* predictions (Figure S4a). Likewise, changing the miRNA binding site in *cmSP*s and *MIM*s changes their predicted RNA secondary structure which may subsequently impact miRNA binding site accessibility and decoy stability (Figure S4b,c). However, target site accessibility did not strongly correlate with decoy efficacy (Figure S4c), where *MIM172* had the lowest accessibility, despite having a strong efficacy (Todesco *et al.*, 2010). Similarly, there was no clear correlation between decoy efficacy and RNA secondary structure, where whether a miRNA binding site was located in a stem or a loop was not indicative of decoy efficacy. Therefore, bioinformatic predictions of these parameters are not a reliable indicator of decoy efficacy.

With regards to a *SP* construct, one possible advantage of having so many miRNA binding sites is that there is more chance of having at least some sites with high accessibility, and this could be the reason why increasing the number of binding sites within a *cmSP* improves efficacy. However, a higher number of miRNA binding sites does not always correlate with a better efficacy as clearly shown by *MIM159* having a stronger efficacy than both *cmSP159* (15×) and STTM159. Clearly, the different contexts that these binding sites are within strongly impact efficacy. Interestingly, the *MIM* context corresponds to the endogenous *IPS1* sequence, an approximately 600 nt nonprotein coding transcript in both dicots and monocots, raising the possibility that features have evolved within these transcripts that facilitate miRNA recognition and inhibition (Franco-Zorrilla *et al.*, 2007).

In conclusion, from our comparison of the different technologies, it appears that no one approach can be equally applied to all miRNAs guaranteeing the strongest inhibition of miRNA activity; optimizing decoy features for inhibiting one miRNA family may potentially not be able to generally be applied to all miRNAs. This likely highlights not only the subtleties between the different miRNA families that remain to be discovered, but also our lack of knowledge of the factors that control the efficacy of these transcripts in being able to be recognized by and subsequently inhibiting the miRNA. Overall, is it likely that the *SP* approach is less reliable than *MIM*s in inducing a strong loss-of-function phenotype; therefore, we do not advocate it as a superior technology, but more of a complementary technology for when a *MIM*/STTM approach only results in a poor efficacy. However, we do advocate that when attempting to inhibit miRNA activity, multiple decoy constructs may need to be evaluated to determine which has the strongest efficacy, so that the desired outcome can be achieved.

Experimental procedures

Plant material and growth conditions

Arabidopsis thaliana ecotype Columbia (Col-0) was used in all experiments and is referred to as wild type. The *mir159a* and *mir159ab* mutant plants are in a Col-0 background and represent T-DNA insertion loss-of-function mutants, which have been described previously (Allen *et al.*, 2007). Plants were grown on soil (Debco Plugger Mix soil mixed with 3.5 g/L Osmocote Extra Mini fertilizer) in 22 °C growth cabinets under long-day photoperiods (16 hours light/ 8 hours dark, 150 μmol/ m^2/sec).

Generation of binary vectors and transgenic plants

All *SP*s and STTMs sequences were synthesized [GenScript (USA) or IDT (USA)] and cloned into the Gateway donor vector pDONR/Zeo (Invitrogen). Synthesized genes were sequenced to verify their integrity and then subcloned into the Gateway compatible destination vector pMDC32 (Curtis and Grossniklaus, 2003) using the Gateway LR Clonase II enzyme mix (Invitrogen) according to the manufacturer's instructions. The artificial target mimics *MIM159* and *MIM165/166* (Todesco *et al.*, 2010) were obtained from the European Arabidopsis Stock Centre (NASC). They were subcloned into pDONR/Zeo using the Gateway BP Clonase II enzyme mix (Invitrogen) according to the manufacturer's instructions and then recombined into pMDC32 through Gateway LR reaction as described above.

All expression vectors were transformed into *Agrobacterium tumefaciens* GV3101 cells by electroporation (Hellens *et al.*, 2000) and then transformed into Col-0 using the floral dip method (Clough and Bent, 1998). *WtSP159*, *cmSP159* and *MIM159* were also transformed into *mir159a*.

For the generation of the binary vector pOp6-*cmSP165/166*, an LR reaction containing pDONR/Zeo-*cmSP165/166*, pEN-L4-pOp6M2-R1, pEN-R2-F-L3 and the destination vector pB7m34GW.0 (Karimi *et al.*, 2007) was carried out, making use of the MultiSite Gateway recombination system (Invitrogen). Similarly, pOp6-GUS was created by carrying out an LR reaction with pEN-L1-S-L2, pEN-L4-pOp6M2-R1, pEN-R2-F-L3 and pB7m34GW.0 according to the manufacturer's instructions. PoP6-*cmSP165/66* and pOp6-GUS were then transformed into *A. tumefaciens* GV3101 and subsequently into the enhancer trap line HET:59a (provided by NASC) by floral dipping as described above.

Free energies (ΔG) of RNA duplexes formed between *SP* transcripts and miRNAs were calculated using the DINAMelt software (http://mfold.rna.albany.edu/?q=DINAMelt/Two-state-melting; Markham and Zuker, 2005, 2008).

Quantitative real-time PCR (qRT-PCR) analysis

Total RNA was extracted from whole plants using TRIzol (Invitrogen) according to the manufacturer's instructions except for the modifications described in Li *et al.* (2014). RQ1 DNase (Promega) was used to treat RNA samples, except those used for TaqMan assays. 20 μg of total RNA was digested in 80 μL reactions according to the protocol, with the addition of RNaseOUT™ Recombinant RNase Inhibitor (Invitrogen) at a concentration of 1 μL/10 μg RNA. Treated RNA was then purified using the Spectrum Plant Total RNA Kit (Sigma) according to the manufacturer's instructions. 1–5 μg of total RNA was used for cDNA synthesis using SuperScript III reverse transcriptase (Invitrogen) with an oligo dT primer (Invitrogen) according to the manufacturer's instructions. The cDNA was diluted 50× in nuclease-free water and used for qRT-PCR as described in Li *et al.* (2014). *CYCLOPHILIN* 5 (At2 g29960) was used to normalize mRNA levels, and the Rotor-Gene Q software (QIAGEN) was used to carry out comparative quantitation. The values for each gene are derived from the average of triplicate assays. Gene-specific

primers are identical to those previously described (Alonso-Peral *et al.*, 2010).

TaqMan assays for mature miRNA analysis

TaqMan MicroRNA Assays (Applied Biosystems) were used to quantitate mature miRNA levels according to the protocol described by Allen *et al.* (2010). Each cDNA was assayed in triplicate on a Rotor-Gene Q real-time PCR machine (QIAGEN) using the same cycling conditions as described above. Expression of mature miRNAs was normalized to *snoR101* and comparative quantitation analysis was carried out using the Rotor-Gene Q software (QIAGEN). The values for each set of triplicates were averaged, and the standard error of the mean (SEM) was calculated. For both qRT-PCR and TaqMan assays, statistically significant changes were determined using Student's *t*-test analysis.

GUS staining

In situ GUS staining was performed using the method described by Jefferson (1987) with the modifications described in Li *et al.*, 2014.

Acknowledgements

We thank the European Arabidopsis Stock Centre NASC for providing the *MIM159* and *MIM165/166* clones, and the HET:59a enhancer trap line, Rob Allen and Ira Deveson for critically reading the manuscript. This research was supported by an Australian Research Council grant DP130103697, and International ANU PhD scholarships to M.R and Y.L.

References

Adenot, X., Elmayan, T., Lauressergues, D., Boutet, S., Bouche, N., Gasciolli, V. and Vaucheret, H. (2006) DRB4-dependent TAS3 trans-acting siRNAs control leaf morphology through AGO7. *Curr. Biol.* **16**, 927–932.

Allen, R.S., Li, J., Stahle, M.I., Dubroué, A., Gubler, F. and Millar, A.A. (2007) Genetic analysis reveals functional redundancy and the major target genes of the *Arabidopsis* miR159 family. *Proc. Natl. Acad. Sci. USA,* **104**, 16371–16376.

Allen, R.S., Li, J., Alonso-Peral, M.M., White, R.G., Gubler, F. and Millar, A.A. (2010) MicroR159 regulation of most conserved targets in *Arabidopsis* has negligible phenotypic effects. *Silence,* **1**, 18.

Alonso-Peral, M.M., Li, J., Li, Y., Allen, R.S., Schnippenkoetter, W., Ohms, S., White, R.G. and Millar, A.A. (2010) The microRNA159-regulated *GAMYB-like* genes inhibit growth and promote programmed cell death in Arabidopsis. *Plant Physiol.* **154**, 757–771.

Chen, H., Jiang, S., Zheng, J. and Lin, Y. (2013) Improving panicle exsertion of rice cytoplasmic male sterile line by combination of artificial microRNA and artificial target mimic. *Plant Biotechnol. J.* **11**, 336–343.

Clough, S.J. and Bent, A.F. (1998) Floral dip: a simplified method for Agrobacterium-mediated transformation of *Arabidopsis* thaliana. *Plant J.* **16**, 735–743.

Craft, J., Samalova, M., Baroux, C., Townley, H., Martinez, A., Jepson, I., Tsiantis, M. and Moore, I. (2005) New pOp/LhG4 vectors for stringent glucocorticoid-dependent transgene expression in Arabidopsis. *Plant J.* **41**, 899–918.

Curtis, M.D. and Grossniklaus, U. (2003) A gateway cloning vector set for high-throughput functional analysis of genes *in planta*. *Plant Physiol.* **133**, 462–469.

Dai, X. and Zhao, P.X. (2011) PsRNATarget: a small RNA target analysis server. *Nucleic Acids Res.* **39**, W155–W159.

Eamens, A.L., Agius, C., Smith, N.A., Waterhouse, P.M. and Wang, M.B. (2011) Efficient silencing of endogenous microRNAs using artificial miRNAs in *Arabidopsis thaliana*. *Mol. Plant,* **4**, 157–170.

Ebert, M.S., Neilson, J.R. and Sharp, P.A. (2007) MicroRNA sponges: competitive inhibitors of small RNAs in mammalian cells. *Nat. Methods,* **4**, 721–726.

Emery, J.F., Floyd, S.K., Alvarez, J., Eshed, Y., Hawker, N.P., Izhaki, A.S., Baum, F. and Bowman, J.L. (2003) Radial patterning of *Arabidopsis* shoots by class III HD-ZIP and KANADI genes. *Curr. Biol.* **13**, 1768–1774.

Franco-Zorrilla, J.M., Valli, A., Todesco, M., Mateos, I., Puga, M.I., Rubio-Somoza, I., Leyva, A., Weigel, D., García, J.A. and Paz-Ares, J. (2007) Target mimicry provides a new mechanism for regulation of microRNA activity. *Nat. Genet.* **39**, 1033–1037.

Garcia, D., Collier, S.A., Byrne, M.E. and Martienssen, R.A. (2006) Specification of leaf polarity in Arabidopsis via the trans-acting siRNA pathway. *Curr. Biol.* **16**, 933–938.

Hansen, T.B., Jensen, T.I., Clausen, B.H., Bramsen, J.B., Finsen, B., Damgaard, C.K. and Kjems, J. (2013) Natural RNA circles function as efficient microRNA sponges. *Nature,* **495**, 384–388.

Hellens, R., Mullineaux, P. and Klee, H. (2000) Technical Focus: a guide to Agrobacterium binary Ti vectors. *Trends Plant Sci.* **5**, 446–451.

Hunter, C., Willmann, M.R., Wu, G., Yoshikawa, M., de la Luz Gutiérrez-Nava, M. and Poethig, S.R. (2006) Trans-acting siRNA-mediated repression of ETTIN and ARF4 regulates heteroblasty in *Arabidopsis*. *Development,* **133**, 2973–2981.

Ivashuta, S., Banks, I.R., Wiggins, B.E., Zhang, Y., Ziegler, T.E., Roberts, J.K. and Heck, G.R. (2011) Regulation of gene expression in plants through miRNA inactivation. *PLoS ONE,* **6**, e21330.

Jefferson, R.A. (1987) Assaying chimeric genes in plants: the GUS gene fusion system. *Plant Mol. Biol. Rep.* **5**, 387–405.

Karimi, M., Bleys, A., Vanderhaeghen, R. and Hilson, P. (2007) Building blocks for plant gene assembly. *Plant Physiol.* **145**, 1183–1191.

Kertesz, M., Iovino, N., Unnerstall, U., Gaul, U. and Segal, E. (2007) The role of target site accessibility in microRNA target recognition. *Nat. Genet.* **39**, 1278–1284.

Li, J. and Millar, A.A. (2013) Expression of a microRNA-resistant target transgene misrepresents the functional significance of the endogenous microRNA:target gene relationship. *Mol. Plant,* **6**, 577–580.

Li, J., Reichel, M. and Millar, A.A. (2014) Determinants beyond both complementarity and cleavage govern microR159 efficacy in *Arabidopsis*. *PLoS Genet.* **10**, e1004232.

Liang, G., He, H., Li, Y., Wang, F. and Yu, D. (2014) Molecular mechanism of microRNA396 mediating pistil development in *Arabidopsis*. *Plant Physiol.* **164**, 249–258.

Markham, N.R. and Zuker, M. (2005) DINAMelt web server for nucleic acid melting prediction. *Nucleic Acids Res.* **33**, W577.

Markham, N.R. and Zuker, M. (2008) UNAFold: software for nucleic acid folding and hybridization. *Methods Mol. Biol.* **453**, 3–31.

McConnell, J.R., Emery, J., Eshed, Y., Bao, N., Bowman, J.L. and Barton, M.K. (2001) Role of PHABULOSA and PHAVOLUTA in determining radial patterning in shoots. *Nature,*, **411**, 709–713.

Poliseno, L., Salmena, L., Zhang, J., Carver, B., Haveman, W.J. and Pandolfi, P.P. (2010) A coding-independent function of gene and pseudogene mRNAs regulates tumour biology. *Nature,* **465**, 1033–1038.

Rutherford, S., Brandizzi, F., Townley, H., Craft, J., Wang, Y., Jepson, I., Martinez, A. and Moore, I. (2005) Improved transcriptional activators and their use in mis-expression traps in *Arabidopsis*. *Plant J.* **43**, 769–788.

Schwab, R., Palatnik, J.F., Riester, M., Schommer, C., Schmid, M. and Weigel, D. (2005) Specific effects of microRNAs on the plant transcriptome. *Dev. Cell,* **8**, 517–527.

Sieber, P., Wellmer, F., Gheyselinck, J., Riechmann, J.L. and Meyerowitz, E.M. (2007) Redundancy and specialization among plant microRNAs: role of the MIR164 family in developmental robustness. *Development,* **134**, 1051–1060.

Sunkar, R., Li, Y.F. and Jagadeeswaran, G. (2012) Functions of microRNAs in plant stress responses. *Trends Plant Sci.* **17**, 196–203.

Todesco, M., Rubio-Somoza, I., Paz-Ares, J. and Weigel, D. (2010) A collection of target mimics for comprehensive analysis of microRNA function in *Arabidopsis thaliana*. *PLoS Genet.* **6**, e1001031.

Vaistij, F.E., Elias, L., George, G.L. and Jones, L. (2010) Suppression of microRNA accumulation via RNA interference in *Arabidopsis thaliana*. *Plant Mol. Biol.* **73**, 391–397.

Voinnet, O. (2009) Origin, biogenesis, and activity of plant microRNAs. *Cell,* **136**, 669–687.

Wu, G., Park, M.Y., Conway, S.R., Wang, J.W., Weigel, D. and Poethig, R.S. (2009) The sequential action of miR156 and miR172 regulates developmental timing in *Arabidopsis*. *Cell,* **138**, 750–759.

Wu, H.J., Wang, Z.M., Wang, M. and Wang, X.J. (2013) Widespread long non-coding RNAs as endogenous target mimics for microRNAs in plants. *Plant Physiol.* **161**, 1875–1884.

Xu, L., Yang, L. and Huang, H. (2007) Transcriptional, post-transcriptional and post-translational regulations of gene expression during leaf polarity formation. *Cell Res.* **17**, 512–519.

Yan, J., Gu, Y., Jia, X., Kang, W., Pan, S., Tang, X., Chen, X. and Tang, G. (2012) Effective small RNA destruction by the expression of a short tandem target mimic in *Arabidopsis*. *Plant Cell,* **24**, 415–427.

Zhou, M. and Luo, H. (2013) MicroRNA-mediated gene regulation: potential applications for plant genetic engineering. *Plant Mol. Biol.* **83**, 59–75.

Supporting information

Additional Supporting information may be found in the online version of this article:

Figure S1 Detailed phenotype of severe *cmSP165/166* and *MIM159* plants.

Figure S2 Analysis of target transcript and miRNA levels in *cmSP165/166* (15x) and *MIM165/166* plants.

Figure S3 Nucleotide sequences of *cmSP165/166*, *MIM165/166* and STTM165/166.

Figure S4 Prediction of RNA secondary structure and miRNA target site accessibility of different decoy constructs.

Table S1 Free energy calculations of the interaction between *cmSPs, MIMs*, STTMs and their corresponding miRNAs.